1 Overview

1.1 Introduction

There is broad agreement in the High Energy Physics community that a linear e^+e^- collider with an initial energy of $E_{cm} = 350$–$500\,\mathrm{GeV}$ and a luminosity above $10^{33}\mathrm{cm}^{-2}\mathrm{s}^{-1}$ is of fundamental importance for the future development of Particle Physics; it is in many respects complementary to the Large Hadron Collider (under construction at CERN), and should be built as the next accelerator facility. The scientific case for a next generation electron-positron collider with a centre-of-mass energy well beyond the reach of the LEP storage ring ($E_{cm} \approx 200\,\mathrm{GeV}$) is presented in part III of this report.

The feasibility of a linear collider has been demonstrated by the successful operation of the SLAC Linear Collider (SLC). However, achieving the requirements for a next generation linear collider is by no means an easy task; in particular, high beam powers and very small spot sizes at the collision point are required to obtain a sufficiently high luminosity. Over the past decade, several groups worldwide have been pursuing different linear collider designs. The fundamental difference between TESLA and other designs is the choice of superconducting accelerating structures. The advantages of superconducting technology (summarised below) are significant and we are convinced that the machine performance potential is unrivaled by other concepts. The same arguments apply in the case of the X-ray Free Electron Laser (FEL), which is an integral part of the TESLA project. The scientific case for the FEL is presented in part V.

A first complete conceptual design of the TESLA facility was published in 1997 [1]. In this report we present the updated design of all accelerator sub-systems, and a summary of our experience gained at the TESLA test facility (TTF).

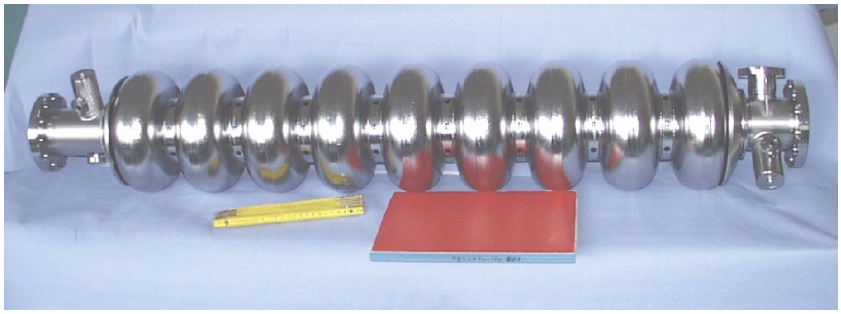

Figure 1.1.1: *The 9-cell niobium cavity for TESLA.*

TESLA uses 9-cell niobium cavities (figure 1.1.1) cooled by superfluid Helium to $T = 2\,\mathrm{K}$ and operating at L-band frequency (1.3 GHz). The design gradient at $E_{cm} = 500\,\mathrm{GeV}$ is $E_{acc} = 23.4\,\mathrm{MV/m}$ and the quality factor $Q_0 = 10^{10}$ (based on the linac layout described in chapter 3). Because the power dissipation in the cavity walls is extremely small, the accelerating field can be produced with long, low peak power RF-pulses; this results in a high RF to beam power transfer efficiency, allowing a high average beam power while keeping the electrical power consumption within acceptable limits ($\sim$100 MW).

The high beam power is one of the ingredients for high luminosity; the second essential point for high luminosity is the extremely small beam size at the interaction point (IP). The relatively low frequency of the TESLA linac is ideally suited for accelerating and *conserving* ultra-small emittance beams. Beam dynamics issues are discussed in detail in section 3.2, but a convincing argument for the choice of low frequencies based on simple scaling laws can be made as follows: the beam accelerated in the linac induces electromagnetic fields (so-called wakefields) which act back on the beam. If the wakefields are too strong, they can degrade the quality of the beam by increasing its energy spread and transverse emittance. The longitudinal and transverse wakefields per unit length of accelerator scale approximately as f^2 and f^3 respectively: hence the wakefields in TESLA ($f = 1.3\,\mathrm{GHz}$) are considerably weaker compared to those of machines based on S-band ($f = 3\,\mathrm{GHz}$) [4] or X-band ($f = 11.4\,\mathrm{GHz}$) [2, 3] technologies. As a result, the emittance dilution can be reduced to acceptable levels in TESLA using relatively relaxed alignment tolerances for the linac components.

The choice of superconducting RF also allows us to use a long RF-pulse (1 ms) and a relatively large bunch spacing (337 ns at $E_{cm} = 500\,\mathrm{GeV}$). Three benefits result directly from this long bunch train:

- A fast (MHz) bunch-to-bunch feedback can be used to correct the orbit within one beam pulse. Such a feedback system will maintain the beams in collision at the IP, making TESLA relatively insensitive to mechanical vibrations which could otherwise lead to serious luminosity reduction.

- A head-on (zero crossing-angle) collision scheme can be used, with large-aperture superconducting quadrupoles in the interaction region.

- In the event of an emergency, a fast safety system can 'turn off' the beam within a fraction of a pulse.

The potential benefits of superconducting RF summarised above have been acknowledged since the beginning of linear collider R&D. However, in the early 1990's, the projected costs based on existing superconducting RF installations were considered too high. The main challenge for TESLA, therefore, was a reduction in the cost per unit accelerating voltage by a large factor, in order to be competitive with conventional linear collider designs. The approach adopted to reduce the cost was to:

- increase the achievable gradients available at that time (5–8 MV/m [5, 6]) by about a factor of four; and

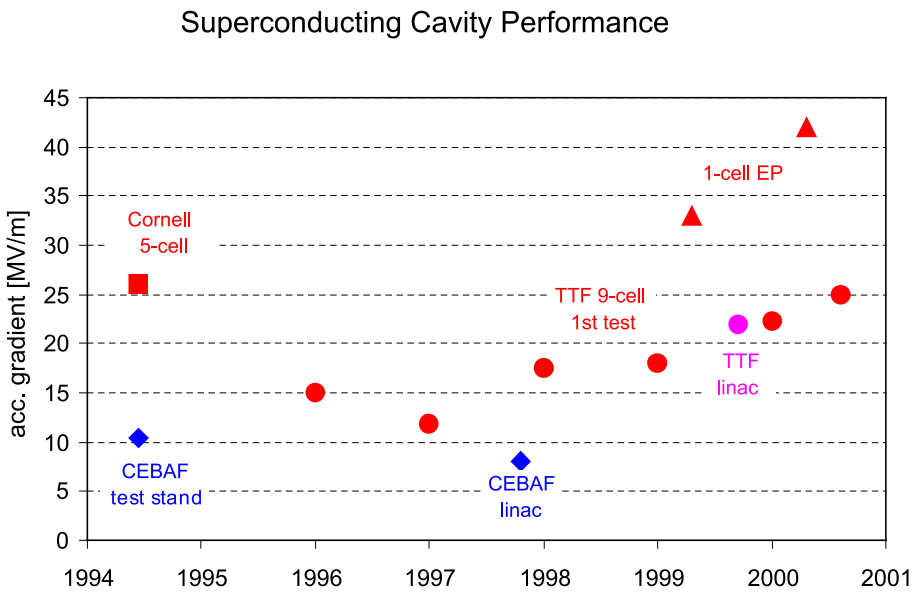

Figure 1.1.2: *Evolution of superconducting cavity performance: red dots show the average gradient achieved with TESLA 9-cell cavities for the years 1995–2000 (first test, no additional processing), the red square shows results for 5-cell cavities at Cornell and the magenta dot depicts the average gradient measured with beam for a complete accelerator module installed at the TTF linac. Red triangles show gradients obtained with electropolished single-cell resonators (see text). Test stand and linac operation results from Jefferson Lab (CEBAF) are included for comparison (blue diamonds).*

- reduce the cost per unit length of the superconducting structures by a similar factor.

In order to demonstrate the feasibility of the high-gradient cavity technology and to create a solid basis for a reliable cost estimate of future large-scale production, the TESLA collaboration decided in 1992 to start an R&D program and to build the TESLA Test Facility (TTF) [7]. The TTF includes the infrastructure for applying different processing techniques to the niobium cavities obtained from industrial production. A detailed overview of the cavity development programme at TTF is given in chapter 2.

In the formative stages of the TESLA collaboration, three 5-cell L-band cavities were built and tested at Cornell, and reached accelerating fields of 26–28 MV/m [8]. To date, more than sixty 9-cell cavities have been processed and tested at TTF. Figure 1.1.2 shows the average gradient obtained in the years 1995–2000. Only data from the first test with cw-RF excitation are included. Several cavities reached higher performance after additional processing, but in view of future mass production, the performance obtained after a cavity has passed through the standard fabrication and treatment procedure may be considered more relevant. The steady improvement of the average gradient over the past years clearly indicates that the high performance cav-

ities required for the 500 GeV collider can now be produced with sufficient reliability. Furthermore, studies carried out together with industry have shown that the required mass production is feasible within the planned time schedule, and that the cost goal is achievable (see chapter 10).

Further progress on the cavity performance has recently been obtained by applying electropolishing to the niobium surface. Test results with single-cell resonators repeatedly show gradients above 30 MV/m [9]. The best single-cell performance obtained to date is $E_{acc} = 42$ MV/m (see chapter 2). First results for 9-cell electropolished cavities also show gradients well above 30 MV/m. We are therefore confident that the cavities in the TESLA linac will be able to operate at a gradient above 30 MV/m, allowing a significant increase in the achievable centre-of-mass energy (section 1.4).

Besides the success of the cavity development programme, the commissioning and operation of the TTF linac has been the second essential milestone reached on our way to demonstrate the feasibility of the TESLA technology. The linac [10] is constructed from accelerator modules similar to those required for the collider, and permits a full integrated system test with beam (section 2.2). We have so far tested three modules and operated the linac for more than 8,000 hours. Each 12 m long module is comprised of a string of eight 9-cell cavities (figure 1.1.3), together with beam focusing and diagnostic components. The highest average accelerating gradient measured for a module was 22 MV/m.

Our baseline design for the 500 GeV machine (chapter 3) is based entirely on the design of components installed and tested at TTF, with the exception of an optimisation of the mechanical layout of the modules (see section 3.3). The modified module improves the fill factor (ratio of active length to total length) and hence reduces the gradient required to reach the design energy within a given site length. A further improvement along the same lines is currently being developed: by grouping several cavities into a so-called superstructure (section 2.1) with minimum inter-cavity spacing, the energy reach of the machine can be maximised while at the same time reducing the cost of the RF-distribution system (reduced number of couplers). However, we have chosen to conservatively base the parameters and cost estimate for the 500 GeV machine on the TTF-like accelerator module, since as of writing, tests of the superstructure are still in preparation.

1.1.1 X-ray Free Electron Laser (FEL)

The concept of using a high energy electron linac for building an X-ray Free Electron Laser (FEL) was first developed at Stanford [11]. Due to its ability to conserve a high beam quality during acceleration, the TESLA linac is an excellent driver for an X-ray FEL. The fascinating research possibilities opened up by such a truely new kind of X-ray source and the layout of the User Facility are summarised in part V of this report. The additional accelerator components required for integration of the Free Electron Laser will be described in chapter 9.

Since the X-ray FEL concept represents a considerable extrapolation of present day FEL technology, it was considered necessary to perform a successful test of the

Figure 1.1.3: *Assembly of a string of eight 9-cell cavities in the clean room at TTF.*

Self Amplified Spontaneous Emission (SASE) FEL concept at the TTF, in a wavelength regime previously unaccessible ($\lambda \approx 100\,\mathrm{nm}$). Lasing was first observed in February 2000, and a number of experimental studies at the TTF-FEL have since been carried out (see section 9.2). An upgrade of the TTF linac to 1 GeV beam energy is in preparation, and will allow a second stage of the FEL to reach 6 nm wavelength. The upgraded facility will be available for users from 2004 onwards, and will allow us to gain the operational and scientific experience needed for the operation of the proposed large-scale X-ray FEL laboratory.

1.1.2 Second interaction region (IR) and further options

Unlike a storage ring collider, a linear collider cannot serve several interaction regions simultaneously with the same beam. It is possible, however, to switch the beam between two experimental stations. We have integrated the option of a second IR in the layout of the TESLA facility. Unlike the primary IR which has a zero crossing angle, the second IR will have a crossing angle of $\sim$34 mrad, and is therefore suitable for the $e\gamma$ and $\gamma\gamma$ collider modes of operation described in part VI, chapter 1. The second IR can also be used for electron-positron collisions, with the same luminosity as the primary IR (assuming that the so-called crab-crossing scheme is used). Electron-electron collisions (at one or both of the IRs) can be provided by reversing magnet polarities and adding a polarised electron source to the (nominal) positron branch of the collider. The expected performance for the $\gamma\gamma$ and e^-e^- modes of operation are included in the discussion of machine parameters in section 1.3.

In addition to collider operation, TESLA also offers options for fixed target physics.

It is possible to accelerate (in parallel with the main collider beam) a low-intensity spin-polarised electron beam which can be deflected into a separate beamline and used for a polarised target experiment (see part VI, chapter 3). Except for the additional experimental beamline and low-current polarised electron source, the impact on the accelerator itself is marginal, since the required additional RF-power is only about 10^{-3} of the nominal power.

If TESLA is built next to the DESY site, the first part of the linac can be used as an injector for the HERA electron ring, which could be operated as a pulse stretcher to deliver a continuous beam at 15–25 GeV for fixed target Nuclear Physics experiments [12]. This option provides a beam with properties very similar to the original ELFE proposal [13] and to a more recent design worked out at CERN [14]. It is described in more detail in part VI, chapter 4.

As a last possible option, the TESLA linac could be connected tangentially to the west straight section of HERA, allowing the (TESLA) electron beam to collide with protons (see part VI, chapter 2). The achievable centre-of-mass energy would exceed the present HERA energy by a factor of three to five. The most serious issue here concerns the achievable luminosity (see for example [15, 16, 17]). More detailed studies are required before a conclusion concerning the feasibility of a linac-ring e-p collider with reasonably high luminosity can be drawn.

1.2 General Layout

A sketch of the overall layout of the TESLA linear collider is shown in figure 1.2.1. In this section, a brief description of each of the sub-systems will be given, beginning with the electron and positron sources.

The electron beam is generated in a polarised laser-driven gun (section 4.2). After a short section of conventional linac, the beam is accelerated to 5 GeV in superconducting structures identical to the ones used for the main linac. The baseline design assumes that the electrons are stored in a damping ring very similar to the one required for the positron beam (see below). A novel concept for a low-emittance flat beam electron gun has recently been suggested [18], which may allow direct production of a beam of suitable quality for collider operation. The obvious cost saving makes the scheme very attractive: however, there are still several questions that need to be addressed, among them whether or not the concept can be used to produce the required *polarised* electrons.

The positron injection system has to provide a total charge of about $5 \cdot 10^{13} e^+$ per beam pulse, which is not realistically feasible with a conventional (electron on thick target) source. Instead, positrons are produced from γ-conversion in a thin target (section 4.3), after which they are preaccelerated in a conventional 200 MeV L-band linac, followed by a 5 GeV superconducting accelerator. The photons are generated by passing the high-energy electron beam through an undulator placed after the main linac, before transporting the beam to the IP. Passage through the undulator causes the energy spread in the electron beam to increase from $0.5 \cdot 10^{-3}$ to $1.5 \cdot 10^{-3}$, with

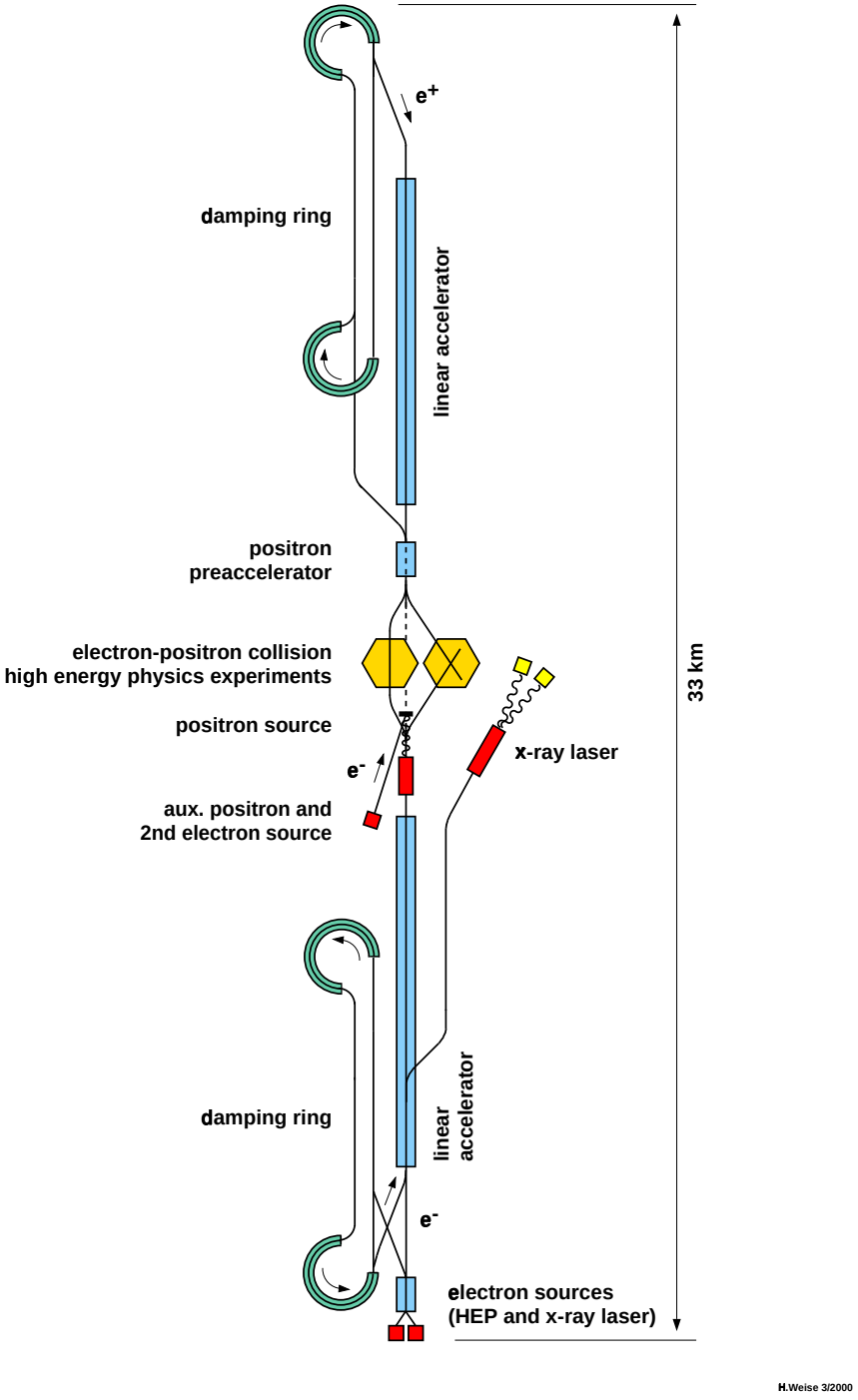

Figure 1.2.1: *Sketch of the overall layout of TESLA.*

an average energy loss of 1.2 %, both of which appear tolerable. Locating the positron source upstream of the IP reflects a design change compared to the system described in [1], where the source was located after the IP in the spent-beam extraction line. Placing the source upstream of the IP has removed the need to collimate a substantial fraction of the high power spent-beam, which had posed technical and radiation safety problems.

The undulator-based positron source requires an electron beam energy greater than 150 GeV for full design positron beam intensity. At centre-of-mass energies below 300 GeV the luminosity is reduced due to a lower positron beam current. If lower energy running at maximum luminosity becomes important, additional electron beam pulses and bypass-beamlines are foreseen to drive the positron source independently from the (lower-energy) beam used for physics.

Besides providing a sufficiently high positron beam intensity, the undulator-based source offers several additional advantages:

- use of a thin target leads to a smaller positron beam with a smaller transverse emittance than from a conventional (thick target) source;
- the considerable investment and operating costs for a high-power electron linac needed in a conventional scheme are avoided;
- production of *polarised* positrons is possible by replacing the planar undulator with a helical undulator.

The polarised positron option is technically more ambitious and is considered a potential upgrade at a later stage of operation. The achievable polarisation ranges from 45% to 60%.

In addition to the main undulator-based source, a low-intensity auxiliary e^+ source will be installed for commissioning and machine study purposes. The auxiliary source should be capable of generating a bunch train of a few percent of the design intensity.

The positron beam is injected into the damping ring at an energy of 5 GeV. The bunch train is stored in the ring in a compressed mode, with the bunch spacing reduced by about a factor of 16; even with this compression, a large ring circumference of about 18 km is still required. To avoid building an additional large ring tunnel, a so-called 'dog bone' design is used (chapter 5). The layout has two 8 km straight sections placed entirely in the main linac tunnel; additional tunnels are only required for the 1 km circumference loops at either end. About 400 m of wiggler section are needed to achieve sufficient damping. Fast kickers are required for compression and decompression of the bunch train at injection and extraction respectively.

Despite its unconventional shape, the damping ring does not exhibit any unusual beam dynamics. The only exception, related to the large ratio of circumference to beam energy, is a large incoherent space charge tune shift. The effect can be significantly reduced, however, by artificially increasing the beam cross-section in the long straight sections.

The two main linear accelerators (chapter 3) are each constructed from roughly ten-thousand one-meter long superconducting cavities. Groups of twelve cavities are installed in a common cryostat (cryomodule); the current design is based on that used in the TTF, modified to be more compact and cost-effective. The cryomodules also contain superconducting magnets for beam focusing and steering, beam position monitors, and higher-order mode absorbers.

The RF-power is generated by some 300 klystrons per linac, each feeding 36 9-cell cavities. The required peak power per klystron is 9.5 MW, including a 10% overhead for correcting phase errors during the beam pulse which arise from Lorentz force detuning and microphonics. The high-voltage pulses for the klystrons are provided by conventional modulators: an alternative option presently under study is the use of superconducting magnet energy storage (SMES) devices, where the pulse energy is stored in the magnetic field of superconducting solenoids. The TESLA RF-system is described in detail in section 3.4.

The cryogenic system for the TESLA linac (section 8.7) is comparable in size and complexity to the one currently under construction for the LHC at CERN. Seven cryogenic plants are foreseen, each one serving a $\sim$5 km long linac subsection. The cooling capacity of the first section of the electron linac is increased to accommodate the higher load from the additional FEL beam pulses.

The beam transport between the linac and the IP (the so-called beam delivery system, described in chapter 7) consists of collimation, beam diagnostics and correction, and final focus sections. The relatively large bunch spacing of 337 ns allows a head-on collision scheme, since the beams can be safely extracted outside of the detector region and before the first parasitic bunch crossing ($\sim$50 m from the IP). Large aperture superconducting quadrupoles can be used in the IR, with one benefit being that collimation requirements upstream for protection of the experiment from background are rather relaxed. With gas scattering practically absent in the TESLA linac and weak wakefields, the expected amount of beam halo which must be collimated is expected to be small: hence background from muons originating at the collimators is unlikely to be a problem. If the loss rate at the collimators exceeds an acceptable limit (e.g. due to mis-steering or other possible failures upstream), the large bunch spacing allows a fast emergency extraction system to send the remainder of the bunch train to the main beam dump.

The design of the final focus system is essentially the same as the Final Focus Test Beam (FFTB) system successfully tested at SLAC [19]. Beam size demagnification and chromatic corrections for the TESLA design parameters are no more ambitious than at the FFTB. The beams can be kept in collision at the IP to a high precision by using a fast bunch-to-bunch feedback, which measures and corrects the beam-beam offset and crossing angle on a time scale small compared to the beam pulse length. A similar system is foreseen after the main linac, to remove possible pulse-to-pulse orbit jitter. If necessary, a fast orbit correction can also be installed at the entrance of the main linac to remove jitter generated in the injection system. A prototype of the orbit feedback system has been installed and successfully tested at the TTF linac [20].

The design of the beam delivery system is optimised for a single head-on interaction

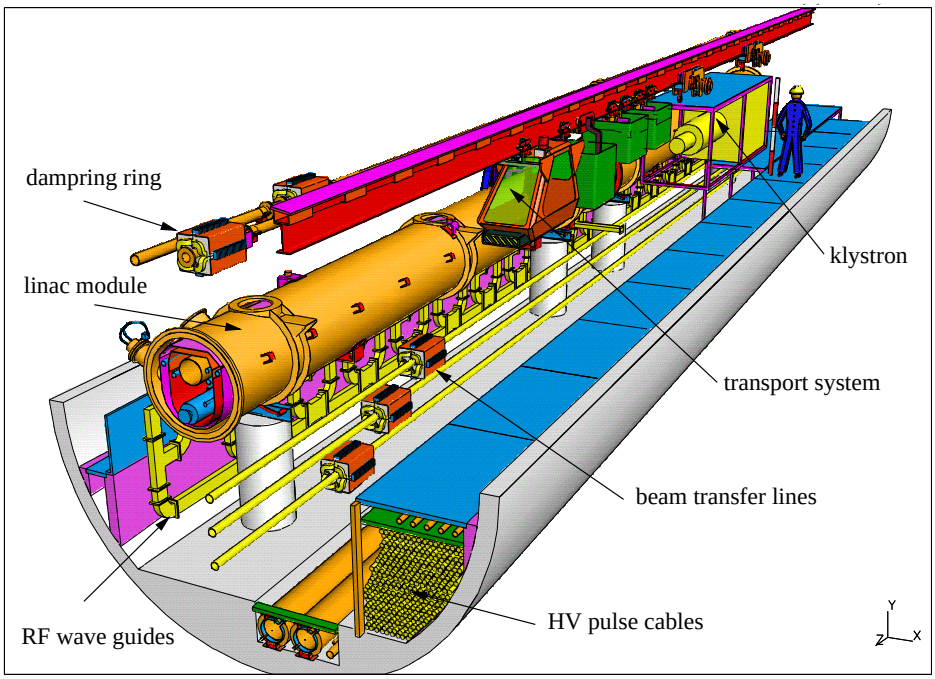

Figure 1.2.2: *Sketch of the 5 m diameter TESLA linac tunnel.*

point. The complete system of ∼3.3 km (linac to linac) will fit into a straight tunnel. All the magnet systems and beamline geometry are designed to allow an upgrade to a beam energy of 400 GeV. As previously mentioned, a second IR with a 34 mrad crossing angle is also foreseen, which could be used for $\gamma\gamma$ or $e^-\gamma$ collisions. On the electron linac side, care has been taken to place the positron source (undulator) upstream of the beam switchyard, so as not to exclude the possibility of e^+e^- collisions at the second IR.

The two linear accelerators as well as the beam delivery system will be installed in an underground tunnel of 5 m diameter (see figure 1.2.2 and section 8.2). A 2000 m^2 experimental hall is foreseen to house the detector; the hall can be extended to house a second detector should the second IR be constructed. Seven additional surface halls are required for the cyrogenic plants, spaced at intervals of about 5 km along the linacs, and are connected to the underground tunnel by access shafts. The halls will also contain the modulators which generate the HV pulses for the klystrons. The pulse transformers are placed in the tunnel close to the klystrons; the long cables required to connect the modulators to the transformers contribute a few % to the total power losses, but it is an advantage to allow access to the modulators for maintenance during machine operation. Exchange of klystrons, however, will require an interruption of the machine operation: with an energy overhead of 2% foreseen in the design, and assuming an average klystron lifetime of 40,000 hours, maintenance breaks of one day every few weeks will be necessary.

The first 3 km long section of the electron linac is used to accelerate the beam

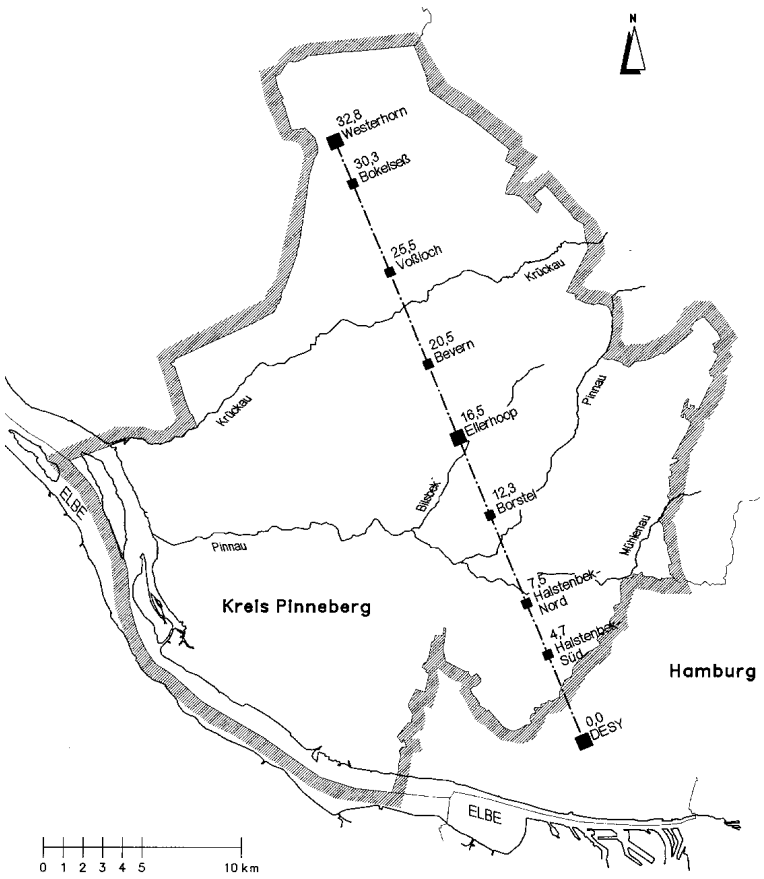

Figure 1.2.3: *The TESLA site North-West of the DESY laboratory.*

which drives the X-ray FEL user facility. This part of the machine operates at 10 Hz — twice the nominal collider repetition rate — alternating from pulse to pulse between collider and FEL mode operation. The accelerating gradient for the FEL beam can be adjusted independently within a range of more than a factor of two (9–23 MV/m). Two extraction points are foreseen at different positions in the linac, supplying beam energies in the range 11–50 GeV to the FEL facility[1]. The extracted beams are transported in two separate transfer lines to the FEL laboratory, which is placed adjacent to the High Energy Physics experimental halls. The FEL beam requires its own low emittance source, low energy pre-accelerator and bunch compression systems. A description of the machine components related to the FEL is given in chapter 9.

Within the TESLA collaboration there is broad agreement that the facility should be constructed at an existing High Energy Physics laboratory to reduce project costs and construction time. Both DESY and FNAL have been considered as possible sites [21]. DESY as the co-ordinating laboratory in the collaboration has taken over the task of working out a detailed plan for the TESLA site North-West of the DESY

[1] Although the top range here is 50 GeV, the present FEL design does not require beam energies above 30 GeV.

laboratory (section 8.2). In this scenario (figure 1.2.3), the linac tunnel starts at the DESY site in a direction tangential to the west straight section of HERA, so as not to exclude the electron-proton linac-ring collider option. The central area is situated about 16 km from the DESY site in a rural part of the North German state (Bundesland) of Schleswig-Holstein, and accommodates both the collider detector hall for Particle Physics and the FEL radiation user facility.

1.3 Parameters for 500 GeV

Besides the centre-of-mass energy of the colliding beams, the second key parameter for a linear collider is the luminosity L, given by

$$L = \frac{n_b N_e^2 f_{rep}}{4\pi\sigma_x^*\sigma_y^*} \times H_D \tag{1.3.1}$$

where

n_b	number of bunches per pulse
N_e	number of electrons (positrons) per bunch
f_{rep}	pulse repetition frequency
$\sigma_{x,y}^*$	horizontal (vertical) beam size at interaction point
H_D	disruption enhancement factor (typically $H_D \approx 2$)

Introducing the average beam power $P_b = E_{cm} n_b N_e f_{rep}$, the luminosity can be written as

$$L = \frac{P_b}{E_{cm}} \times \frac{N_e}{4\pi\sigma_x^*\sigma_y^*} \times H_D \tag{1.3.2}$$

An important constraint on the choice of IP parameters is the effect of beamstrahlung: the particles emit hard synchrotron radiation in the strong electromagnetic space-charge field of the opposing bunch. The average fractional beam energy loss from beamstrahlung is approximately given by [22]:

$$\delta_E \approx 0.86 \frac{r_e^3 N_e^2 \gamma}{\sigma_z(\sigma_x^* + \sigma_y^*)^2} \tag{1.3.3}$$

where

r_e	the classical electron radius
γ	relativistic factor E_{beam}/m_0c^2

Beamstrahlung causes a reduction and a spread of the collision energy and can lead to background in the detector. The energy loss δ_E is therefore typically limited to a few percent. By choosing a large aspect ratio $R = \sigma_x^*/\sigma_y^* >> 1$, δ_E becomes independent of the vertical beam size and the luminosity can be increased by making σ_y^* as small as possible. Since $\sigma_y^* = (\varepsilon_{y,N}\beta_y^*/\gamma)^{1/2}$, this is achieved by a small vertical beta function at the IP (β_y^*) and a small normalised vertical emittance ($\varepsilon_{y,N}$). The lower limit on β_y^* is

given by the bunch length ('hourglass effect'); setting $\beta_y^* = \sigma_z$, the luminosity can be expressed as:

$$L \approx 5.74 \cdot 10^{20} \mathrm{m}^{-3/2} \times \frac{P_b}{E_{cm}} \times \left(\frac{\delta_E}{\varepsilon_{y,N}} \right)^{1/2} \times H_D \tag{1.3.4}$$

The advantages of low-frequency superconducting RF technology have already been mentioned: high RF- to beam-power efficiency; extremely small wakefields and associated linac emittance growth; fast intra-bunch feedback systems. Making use of these unique features has led to a parameter set (table 1.3.1) which clearly demonstrates TESLA's potential for high luminosity. In comparison with the earlier design [1], we achieve about a factor of five improvement in the luminosity, while maintaining a low level of beamstrahlung. The feasibility of this higher performance is supported by a careful investigation and — where necessary — optimisation of the machine subsystems.

1.3.1 Electron-electron and $\gamma\gamma$ collisions

The head-on e^+e^- interaction region can also be operated in e^-e^- mode. The disadvantage here is that the luminosity enhancement arising from self-focusing for oppositely charged bunches turns into a de-focusing effect for like charges, with $H_D < 1$. Assuming identical beam parameters, we find a luminosity seven times smaller [23] than for the e^+e^- mode (see table 1.3.1).

The photon collider option, where the electrons are converted into high energy photons by interaction with a laser beam just upstream of the IP, requires construction of the second interaction region with the large crossing angle. Unlike the e^+e^- case, the beamstrahlung constraint is not present for $\gamma\gamma$ collisions, and the horizontal beam size at the IP can be reduced still further. Table 1.3.2 lists a possible $\gamma\gamma$ parameter set which reflects the lack of the beamstrahlung constraint: the horizontal emittance is at the limit achievable with the present damping ring design, while the IP beta-functions are compatible with a final focus system design similar to the e^+e^- collider version (except, of course, for the crossing angle). Additional improvements are conceivable, but require further design studies of these sub-systems. Crab-crossing is assumed to avoid a luminosity reduction caused by the crossing angle. The actual usable $\gamma\gamma$ luminosity is smaller than the geometric value by an order of magnitude, since not all the electrons are converted by Compton scattering, and only part of the luminosity spectrum is within a few percent of the peak collision energy. For more details on the photon collider, see chapter 1 in part VI.

1.4 Energy Upgrade Potential

The length of the machine must be increased to achieve centre-of-mass energies above $\sim$1 TeV. However, a significant energy upgrade is possible within the site length for the current 500 GeV design, since:

		TESLA-500
Accelerating gradient	E_{acc} [MV/m]	23.4
RF-frequency	f_{RF} [GHz]	1.3
Fill factor		0.747
Total site length	L_{tot} [km]	33
Active length	[km]	21.8
No. of accelerator structures		21024
No. of klystrons		584
Klystron peak power	[MW]	9.5
Repetition rate	f_{rep} [Hz]	5
Beam pulse length	T_P [μs]	950
RF-pulse length	T_{RF} [μs]	1370
No. of bunches per pulse	n_b	2820
Bunch spacing	Δt_b [ns]	337
Charge per bunch	N_e [10^{10}]	2
Emittance at IP	$\gamma\varepsilon_{x,y}$ [10^{-6}m]	10, 0.03
Beta at IP	$\beta^*_{x,y}$ [mm]	15, 0.4
Beam size at IP	$\sigma^*_{x,y}$ [nm]	553, 5
Bunch length at IP	σ_z [mm]	0.3
Beamstrahlung	δ_E [%]	3.2
Luminosity	L_{e+e-} [10^{34}cm^{-2}s^{-1}]	3.4
Power per beam	$P_b/2$ [MW]	11.3
Two-linac primary electric power (main linac RF and cryogenic systems)	P_{AC} [MW]	97
e^-e^- collision mode:		
Beamstrahlung	$\delta_{E,e-e-}$ [%]	2.0
Luminosity	L_{e-e-} [10^{34}cm^{-2}s^{-1}]	0.47

Table 1.3.1: *TESLA parameters for the $E_{cm} = 500\,GeV$ baseline design. The machine length includes a 2% overhead for energy management. The klystron power and primary electric power quoted include a 10% regulation reserve.*

- Building the linac with superstructures (section 2.1) improves the fill factor — and hence the maximum energy for a fixed accelerating gradient and site length — by about 6%.

- The fundamental limit for the gradient in niobium structures at 2 K is above 50 MV/m, and at TTF several 9-cell cavities have already reached gradients around 30 MV/m. Electropolishing followed by low-temperature bake-out has yielded systematically high performance single-cell cavities (section 2.1), with gradients up to 42 MV/m.

- The Lorentz force detuning (which increases as the square of the accelerating

		TESLA-500,$\gamma\gamma$
Repetition rate	f_{rep} [Hz]	5
Beam pulse length	T_P [μs]	950
RF-pulse length	T_{RF} [μs]	1370
No. of bunches per pulse	n_b	2820
Bunch spacing	Δt_b [ns]	337
Charge per bunch	N_e [10^{10}]	2
Emittance at IP	$\gamma\varepsilon_{x,y}$ [10^{-6}m]	3, 0.03
Beta at IP	$\beta^*_{x,y}$ [mm]	4, 0.4
Beam size at IP	$\sigma^*_{x,y}$ [nm]	157, 5
Bunch length at IP	σ_z [mm]	0.3
Geometric luminosity	L_{geom} [10^{34}cm^{-2}s^{-1}]	5.8
Effective $\gamma\gamma$ luminosity	$L_{\gamma\gamma}$ [10^{34}cm^{-2}s^{-1}]	0.6

Table 1.3.2: *Beam parameters for the $\gamma\gamma$ option. The effective luminosity takes into account only the high energy peak of the luminosity spectrum ($E_{cm,\gamma\gamma} \approx 400\,GeV$), see part VI, chapter 1 for details.*

gradient) can be compensated by active mechanical stabilisation using fast piezo tuners; this reduces the need to increase the regulation RF-power overhead at higher gradients. The method was successfully demonstrated at the TTF.

As a reasonable estimate for the maximum gradient in the TESLA linac we assume $E_{acc} = 35\,\mathrm{MV/m}$ at $Q_0 = 5{\cdot}10^9$. Using superstructures, the energy reach of the machine is $E_{cm} = 800\,\mathrm{GeV}$. A parameter set for this energy is shown in table 1.4.1. The beam delivery system and the magnets in the main linac are designed to be compatible with operation up to 400 GeV beam energy. Obtaining high luminosity at maximum energy requires upgrading of the cryogenic plants (approximately doubling the 2K cooling capacity) and of the RF system (doubling the number of RF stations).

It should be noted that operation above the 500 GeV reference energy is already possible without any hardware modification. The cooling plant capacity has a 50% overhead in the baseline design, which allows an increase of the gradient by 20–30%[1], depending on the variation of Q_0 versus g. With constant RF-power, the beam current decreases as $I_b \propto 1/g$; this effect is counter-balanced by a stronger adiabatic damping of the emittance, so that one might expect a constant luminosity. However, since the cavity filling time increases as $g/I_b \propto g^2$, the beam pulse length and thus the luminosity goes down, putting a reasonable upper limit on the initial energy reach of the machine at about 650 GeV.

[1]Only the RF wall losses scale as g^2/Q_0, the other contributions to the 2 K load (static losses, wakefields, about one half of the total load) remain unchanged.

		TESLA-800
Accelerating gradient	E_{acc} [MV/m]	35
Fill factor		0.79
Repetition rate	f_{rep} [Hz]	4
Beam pulse length	T_P [μs]	860
No. of bunches per pulse	n_b	4886
Bunch spacing	Δt_b [ns]	176
Charge per bunch	N_e [10^{10}]	1.4
Emittance at IP	$\gamma\varepsilon_{x,y}$ [10^{-6}m]	8, 0.015
Beta at IP	$\beta^*_{x,y}$ [mm]	15, 0.4
Beam size at IP	$\sigma^*_{x,y}$ [nm]	391, 2.8
Bunch length at IP	σ_z [mm]	0.3
Beamstrahlung	δ_E [%]	4.3
Luminosity	L [10^{34}cm^{-2}s^{-1}]	5.8
No. of klystrons		1240
Power per beam	$P_b/2$ [MW]	17
Two-linac primary electric power	P_{AC} [MW]	≈150

Table 1.4.1: *TESLA parameters for an upgrade to 800 GeV. It is assumed that the linac is built with 2×9-cell superstructures and the RF-power has been doubled (see text).*

Bibliography

[1] R. Brinkmann, G. Materlik, J. Roßbach and A. Wagner (eds.), *Conceptual Design of a 500 GeV e+e- Linear Collider with Integrated X-ray Laser Facility*, DESY-97-048 and ECFA-97-182, 1997, chapter 3: http://www.desy.de/lc-cdr/tesla/tesla.html.

[2] *Zeroth Order Design Report for the Next Linear Collider*, SLAC Report 474, 1996.

[3] *JLC Design Study*, KEK Report 97-1, 1997.

[4] Chapter 4 in ref. [1]: http://www.desy.de/lc-cdr/s-band/s-band.html.

[5] Y. Kimura, *Status of TRISTAN*, Proc. XVth Conf. on High Energy Accelerators, Hamburg, 1992, Vol. I, p. 72.

[6] C. E. Reece, *Operating Experience with Superconducting Cavities at Jefferson Lab*, Part. Acc. **60** (1998) 43.

[7] *Proposal for a TESLA Test Facility*, DESY TESLA-93-01, 1992.

[8] C. Crawford et al., *High Gradients in Linear Collider Superconducting Accelerator Cavities by High Pulsed Power to Suppress Field Emission*, Part. Acc. **49** (1995) 1.

[9] E. Kako et al., *Improvement of Cavity Performance by Electro-Polishing in the 1.3 GHz Nb Superconducting Cavities*, Proc. Part. Acc. Conf., New York 1999, Vol. I, p. 432.

[10] D. A. Edwards (ed.), *TESLA Test Facility Linac - Design Report*, DESY TESLA-95-01, 1995.

[11] *Linac Coherent Light Source (LCLS) Design Study Report*, SLAC-R-521, 1998.

[12] N. D'Hose et al., *Prospects of Hadron and Quark Physics with Electromagnetic Probes*, Proc. of Saint-Malo Workshop, Nucl. Phys. **A622** (1997) 1c - 389c.

[13] J.M. De Conto (ed.), *Electron Laboratory for Europe - Accelerator Technical Proposal*, 1993.

[14] H. Burkhardt (ed.) et al., *ELFE at CERN*, CERN report 99-10, 1999.

[15] M. Tigner, B. H. Wiik and F. Willeke, Proc. Particle Accelerator Conf., San Francisco 1991, Vol. 5, p. 2910.

[16] A. K. Ciftci et al., *Linac-Ring Type Colliders: Fourth Way to TeV Scale*, DESY-97-239, 1997.

[17] R. Brinkmann, *Interaction Region and Luminosity Limitations for the TESLA/HERA e/p Collider*, DESY-M-97-05, 1997.

[18] R. Brinkmann, Y. Derbenev and K. Flöttmann, *A Low Emittance, Flat Beam Electron Source for Linear Colliders*, Proc. 7^{th} EPAC, Vienna 2000, p. 453.

[19] D. Burke for the FFTB Collaboration, *Results from the Final Focus Test Beam*, Proc. 4^{th} EPAC, London 1994, Vol. I, p. 23.

[20] H.-T. Duhme et al., *Feedbackelektronik TTF*, Proc. DESY Beschleuniger-Betriebsseminar, Grömitz 2000, DESY M-00-05, p. 171.

[21] Sections 3.10.2 and 3.10.11 in ref. [1].

[22] P. Chen and K. Yokoya, *Beam-Beam Phenomena in Linear Colliders*, KEK-report 91-2, 1991.

[23] I. Reyzl and S. Schreiber, *Luminosity Issues for the e^-e^- Option of the TESLA Linear Collider*, Proc. 7^{th} EPAC, Vienna 2000, p. 498.